Journal of Scientific & Industrial Research
Vol. 84, October 2025, pp. 1076-1087
DOI: 10.56042/jsir.v84i10.12955

High Gain Microstrip Patch Antenna using Frequency Selective Surface for 5G Energy Harvesting Applications

Bilal Salman Taha[1]*, Zeti Akma Rhazali[1], Jahariah Binti Sampe[2] & Norun Farihah Abdul Malek[3]

[1]Department of Electrical and Electronics Engineering, Universiti Tenaga Nasional (UNITEN), 43000 Kajang, Selangor, Malaysia

[2]Institute of Microengineering and Nanoelectronics, Universiti Kebangsaan Malaysia, 43600 UKM Bangi, Selangor, Malaysia

[3]Department of Electrical and Computer Engineering, Kulliyyah of Engineering, International Islamic University Malaysia, Jalan Gombak, 53100 Kuala Lumpur, Malaysia

Received 03 August 2024; revised 25 April 2025; accepted 04 September 2025

This study introduces a novel microwave power transmission method designed to wirelessly power electronic devices, addressing the issues associated with energy storage and wired power sources. The antenna, fabricated using Roger's RT/5880 substrate measuring 50 × 50 × 1.575 mm, functions within the 3.4 – 3.6 GHz C-band frequency range. The design has been tuned for a broad response and improved axial ratio, resonating throughout a bandwidth of 3.2 – 6.2 GHz, appropriate for WLAN, WiMAX, and 5G applications, with an average gain of 5 dBi. A technique for enhancing the gain of the monopole antenna was employed, utilizing a single-layer 4 × 4 metallic Frequency Selective Surface (FSS) reflector, which produced a band-stop filter response throughout a frequency range of 0.5 – 7 GHz and attained an antenna gain of 10 dB. Additionally, a rectifier circuit was incorporated to enhance power conversion efficiency and output voltage, employing SMD-Schottky diode type HSMS-2850-TR1 components that optimize the design and minimize its size. The rectifier circuit demonstrates an efficiency of 64.5% at an input power of 12 dBm with a 2 kΩ resistive load, producing a maximum voltage of 3.5 V with an input power of 13 dBm and a 10 kΩ load. This design enables the rectenna to operate efficiently in diverse contexts, providing a Power Dynamic Range (PDR) of (−30 to 30) dBm, ensuring a reliable power supply for devices even in low-power conditions. This technique is ideally suited for energizing a range of wireless sensors and other IoT applications

Keywords: 5G Communications, Energy harvesting, FSS reflector, MP antenna, Rectifier circuit

Introduction

Analog voice communication marked the beginning of the first generation of mobile communication in the 1980s.(1) By introducing digital voice and SMS text messaging, the second-generation enhanced network capacity and voice quality.[2] The third-generation brought internet and mobile data access.[3] While the fourth-generation improved network capabilities with high-speed internet and LTE.[4] For upcoming technologies, the fifth generation (5G) is anticipated to offer high speed, low latency, and large band up to 20 Gbps.[5] Power generation has been transformed by 5G mobile communications, offering high-frequency millimetre waves and massive MIMO Multiple Input, Multiple Output technology.[6] Which convert ambient wireless radio frequency energy into DC voltage. In order to support the IoT concept, this technology is essential for energizing low-power devices like wearables and IoT sensors. It allows sensor deployments at distant places, decreases replacement cycles, and increases device battery life. 5G wireless energy harvesting offers low environmental impact and energy efficiency, which promotes the development of green technologies.[7]

Because of their small size, low profile, and simplicity of integration with electronic circuits, Microstrip Patch (MP) antennas are essential in wireless communication systems. Radar systems, satellite communications, and mobile devices all use them.[8] In RF energy harvesting, MP antennas are anticipated to be crucial because they effectively capture ambient radio frequency signals and transform them into DC power for low-energy devices. They are perfect for creating battery-free, self-sustaining devices in remote areas because of their high efficiency and wideband capabilities, which also save maintenance costs and increase system reliability.[9,10]

*Author for Correspondence
E-mail: PE21373@student.uniten.edu.my; belalsal@yahoo.com

By integrating the FSS layer for RF energy harvesting, this work seeks to enhance the performance evaluation of a square MP antenna design. By improving the antenna's efficiency, gain, and bandwidth, the study seeks to fill a major research gap. In order to increase the antenna's efficiency and adaptability under varied wireless settings, the study will make use of sophisticated modeling tools and design approaches. To the knowledge of the authors, a few studies have been conducted on the impact of feeding techniques, FSS designs, and substrate materials on overall MPA performance. In addition to creating 5G technologies, the project intends to scale these concepts for broader applications in the commercial, academic, and (ISM) domains. Through improved impedance matching and radiation efficiency, the design is crucial for raising the effectiveness and dependability of RF energy harvesting. Effective at manipulating Radio Frequency (RF) transmissions, Frequency Selective Surfaces (FSSs) are conductive structures on dielectric substrates that filter and control electromagnetic waves at partial frequencies. They are essential components for modern communication systems.[11] In 5G, RF energy harvesting can be greatly improved by integrating FSS with MP antennas. Because periodic patterns resonate at particular frequencies, the antenna's performance can be greatly enhanced by concentrating and directing incident radio frequency energy.[12] Compact and portable appliances are made possible by FSS, which increases MP antenna gain and directivity, reduces interference, guarantees maximum signal reception, and helps to miniaturize and optimize the complete energy-harvesting system.[13] Finally, by increasing MP antenna gains, FSSs can open the door for effective 5G RF energy harvesting technologies, enabling self-powered, sustainable wireless devices and removing obstacles to the adoption of IoT.[14]

Previous studies have mainly integrated FSS layers with antennas, but their use in wireless energy harvesting remains limited. This work introduces a novel integration of the FSS layer with both antenna and rectifier to boost power conversion efficiency, especially under low-power conditions where output voltage often drops. The FSS layer improves rectifier performance by enhancing RF-to-DC conversion and strengthening the antenna's gain and radiation pattern across a wide frequency range, achieving up to 10 dB directivity for better RF energy capture.[15,16]

This study introduces a square MP antenna integrated with an FSS layer to enhance RF energy harvesting. The FSS layer improves impedance matching, gain, and bandwidth by optimizing current distribution and resonance control. Advanced simulations and design techniques are used to boost efficiency and rectifier performance, particularly under low-power conditions. The design is evaluated against conventional antennas and across different substrates and feeding methods, showing superior performance. Its scalability makes it suitable for various applications, including 5G and ISM, addressing key gaps in existing antenna research.

Proposed Methodology

The proposed methodology presents a structured approach to designing a compact, high-gain microstrip patch antenna integrated with FSS to improve performance in 5G energy-harvesting applications. The process began with a theoretical analysis of antenna fundamentals and FSS behavior to explore how their integration could increase bandwidth, gain, and impedance matching. A circular patch configuration was selected for its simplicity and stable radiation characteristics, while an FSS layer was introduced beneath the antenna to act as a reflective surface, redirecting the radiated waves in phase and improving radiation efficiency. The design and optimization were done using the CST Microwave Studio, where critical parameters such as substrate thickness, dielectric constant and feeding conditions were adjusted for optimal results. The Rogers RT/5880 substrate was chosen due to its low dielectric loss and excellent stability at high frequencies. The FSS unit cells were patterned in a periodic 4 × 4 square-loop arrangement with an optimized air gap to achieve constructive interference and enhance directivity. Following the simulation phase, antenna and FSS prototypes were fabricated using precision photolithography, and experimental testing was performed in an anechoic chamber to validate the simulation accuracy. Key performance parameters, including return loss, bandwidth and gain, demonstrated close agreement between measured and simulated data, confirming the reliability of the design. Additionally, an initial rectifier circuit was designed using ADS software to assess the RF-to-DC conversion efficiency, supporting the suitability of the antenna for energy-harvesting systems. Overall, the methodology integrates theoretical design, numerical optimization, and experimental validation.

Antenna Design, Optimization and Fabrication

This section presents the fundamental procedure for the proposed antenna design, optimization, and fabrication. To develop the proposed design, several crucial steps must be taken into account. The first step is the design of a circular shaped regular MP antenna. In order to design the regular antenna, a list of the function parameters should be selected, as depicted in Table 1.

Rogers RT/5880 is selected for its superior RF properties, including low dielectric loss, stable dielectric constant ($\varepsilon_r \approx 2.2$), and excellent high-frequency performance, making it ideal for microwave and millimeter-wave applications such as radar, satellite, and 5G systems. Its low signal attenuation and moisture absorption (~0.02%) further enhance environmental reliability, outperforming alternatives like FR4 at high frequencies. In this study, line feeding is used to optimize coupling and impedance matching, with R_{in} maximized at the patch edges and minimized at the centre. Antenna dimensions are calculated using MATLAB based on standard design equations.[17,18]

$$W_{sub} = \frac{6\times10^8}{2f_o\sqrt{(\varepsilon_r+1)0.5}} \quad \ldots (1)$$

$$\varepsilon_{reff} = \frac{\varepsilon_r+1}{2} + \frac{\varepsilon_r-1}{2}\left[1+12\frac{h}{W}\right]^{-\frac{1}{2}} \quad \ldots (2)$$

$$\Delta L = 0.412h\frac{(\varepsilon_{reff}+0.3)\left[\frac{W}{h}+0.264\right]}{(\varepsilon_{reff}-0.258)\left[\frac{W}{h}+0.8\right]} \quad \ldots (3)$$

$$L_{sub} = \frac{2}{2f_o\sqrt{\varepsilon_{reff}}\sqrt{\mu\varepsilon}} - 2\Delta L \quad \ldots (4)$$

$$W_{feed} = \frac{2h}{\pi}\left\{\frac{377\pi}{2Z_0\sqrt{\varepsilon_r}} - 1 - \ln\left(2\frac{377\pi}{2Z_0\sqrt{\varepsilon_r}} - 1\right) + \frac{\varepsilon_r-1}{2\varepsilon_r}\left[\ln\left(\frac{377\pi}{2Z_0\sqrt{\varepsilon_r}} - 1\right) + 0.39 - \left(\frac{0.61}{\varepsilon_r}\right)\right]\right\} \quad \ldots (5)$$

$$a = \frac{F}{\sqrt{\left\{1+\frac{2h}{\pi\varepsilon_r F\left(\ln\left(\frac{\pi F}{2h}\right)+1.7726\right)}\right\}}} \quad \ldots (6)$$

$$F = \frac{8.791\times10^9}{f_o\sqrt{\varepsilon_r}} \quad \ldots (7)$$

Table 1 — Major parameters for the MP antenna design

Parameters	Definition
Operation frequency (f_o)	3.5 and 5.8 GHz
Substrate type	Rogers RT/5880
Thickness of substrate (h)	1.575 mm
Dielectric constant (ε_r)	2.2
Input impedance (R_{in})	50Ω
Metal thickness	0.035 mm

$$a_e = a\sqrt{1+\left(\frac{2h}{\pi\varepsilon_r a}\right)\left(\ln\left(\frac{\pi a}{2h}\right)+1.7726\right]\right)} \quad \ldots (8)$$

where, W_{sub} is the width for the substrate, ε_{reff} is the effective relative permittivity, ΔL is the length extension, L_{sub} is the substrate length, W_{feed} is the feed line width, a_e is the patch radius and Z_0 is the input impedance.

The next step, after calculating the MP antenna dimensions, is to start the simulation process through the utilization of the Computer Simulation Technology (CST) software, which provides the finite integration technique. The primary design is circular in shape, as shown in Fig.1.

The proposed design addresses the narrow bandwidth issue in MP antennas by using a low dielectric constant and optimized substrate thickness, along with coupled resonators to enhance gain and bandwidth. Advanced feeding techniques like proximity and aperture coupling improve impedance matching over a wider frequency range. Geometric modifications, such as reshaping the coplanar ground plane and introducing a flare angle near the feed gap support higher-order mode resonance and bandwidth enhancement, particularly for low-band 5G energy harvesting. Additional improvements include an inset feed for better matching and an elliptical patch extension to increase the radiating patch's effective length, resulting in improved gain (up to 5.65 dB) and return loss, as shown in Fig. 2.

Proposed FSS Unit Cell Design

The proposed design for the FSS is completely mad by using the CST antenna simulation software, Fig. 3 collectively presents the designed FSS unit cell together with its simulated electromagnetic responses under different conditions. Simulated unit cell FSS as shown in Fig. 3(a) illustrates the geometry and

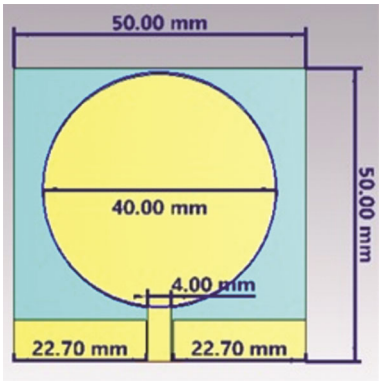

Fig. 1 — Simulated circular MP antenna in CST

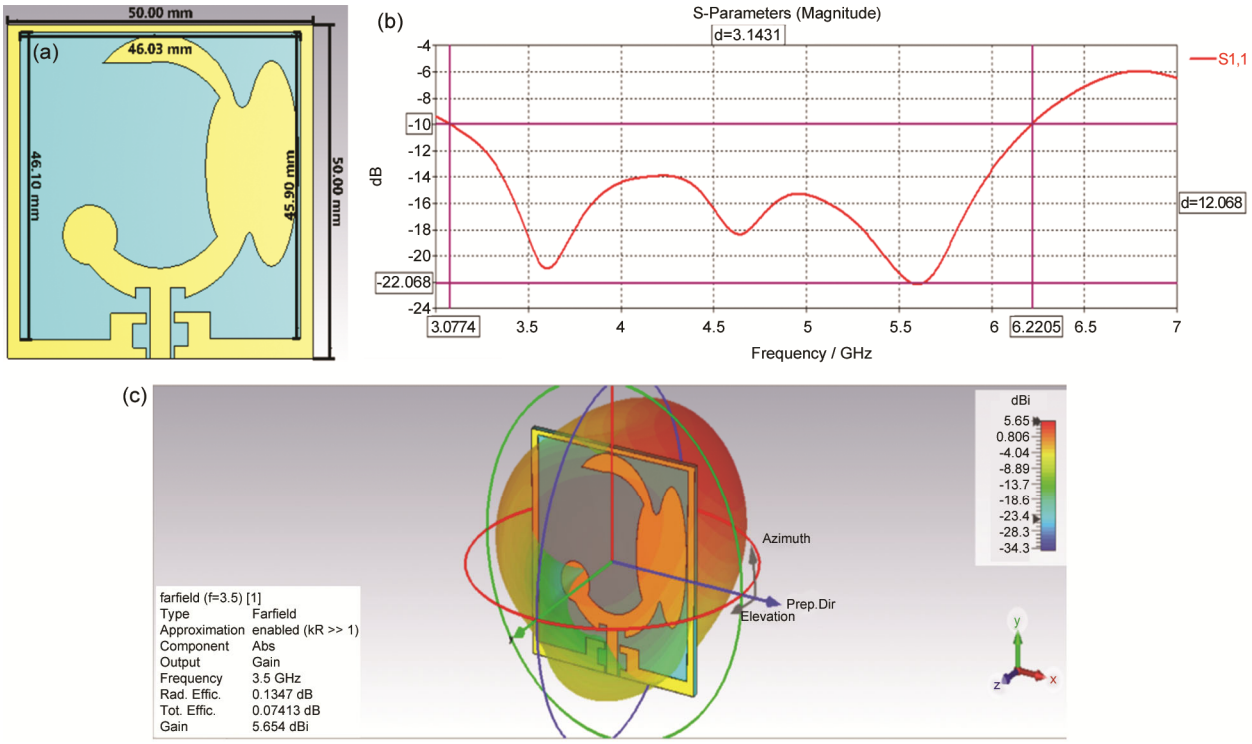

Fig. 2 — Proposed wideband antenna with simulation results: (a) design, (b) S_{11}, (c) Gain for MP antenna

dimensions of the single unit cell, calculated using the formulations reported by Kumar *et al.*[19] The periodic arrangement of symmetric square rings provides the structural foundation for the filtering behavior observed in the subsequent results. S-parameters for single unit cell shown in Fig. 3(b) are the transmission (S_{12}) and reflection (S_{11}) coefficients at normal incidence. Here, the symmetric configuration produces nearly identical co-polarized responses for TE and TM modes. At the design frequency of 3.5 GHz, the filtering is particularly strong, with S_{12} dropping to approximately −72 dB and S_{11} reduced to about −0.0003 dB. Effect of varying theta (θ) on TE mode transmission as shown in Fig. 3(c) demonstrates the angular response for TE polarization. As θ increases from 0° to 80°, the resonant frequency gradually shifts, a behavior attributed to the reduction in the tangential component of the wave vector at higher angles.[20,21] Effect of varying θ on TM mode transmission as shown in Fig. 3(d) presents the corresponding results for TM polarization, where a similar angular dependence is observed. Taken together, the results confirm that the proposed FSS exhibits strong frequency selectivity at normal incidence while maintaining polarization-insensitive performance and stability under oblique incidence, thereby underscoring the robustness of the design.

Resonance frequencies for the TM polarized waves moved to the left as the incident angle decreased, while the incident angle increased, the transmission peaks reduced. These numerical findings demonstrate that the suggested unit cell transmission performed fairly good polarized waves over (50°) angles of incidence with 80% transmissions for both the TE and TM.

For both TE and TM polarized incident waves, there were differences in the 10 dB reflection bandwidth of up to 80° depending on the incident angle. Multiple resonance effects are increasing the bandwidth by 50° of incident angle. The S_{12} response for both the TE and TM modes is equal at a given angle of incidence. Therefore, in terms of a broad bandwidth, it can be stated that the final dual layer structure that has been presented is polarization independent.

The setup of the suggested MP antenna in conjunction with the 4 × 4 FSS substrate is illustrated in Fig. 4(a). The FSS array and a conventional modified circular MP antenna are used in this study. The antennas' proven passband properties indicate that they operate as transparent surfaces to incoming electromagnetic waves inside the study band.

A printed 4 × 4 unit-cell array that forms the FSS array is cascaded and strategically positioned directly

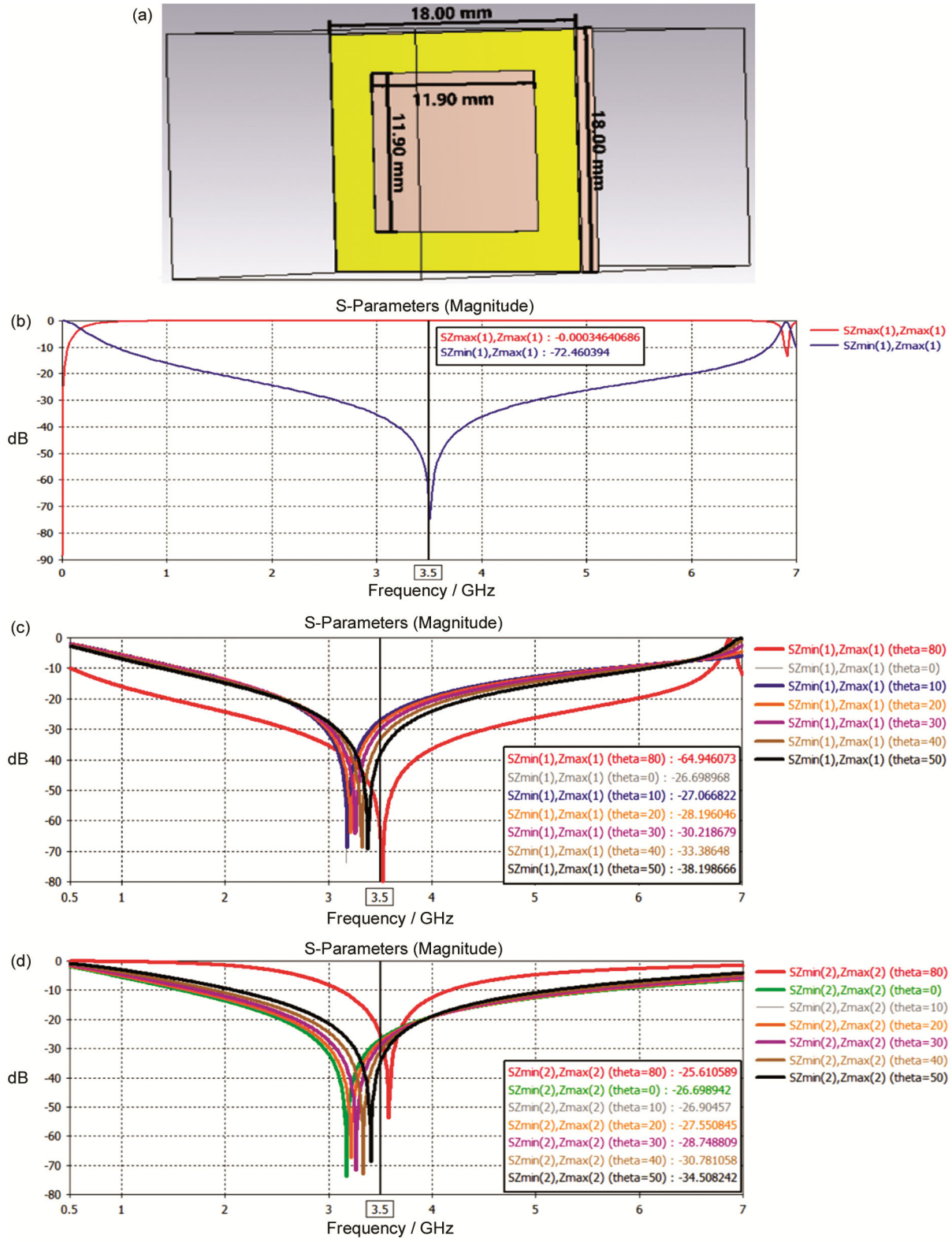

Fig. 3 — Simulated FSS unit cell and its electromagnetic response: (a) Unit cell FSS, (b) S-parameters, (c) Effect of θ variation on TE transmission, (d) TM mode transmission under varying θ

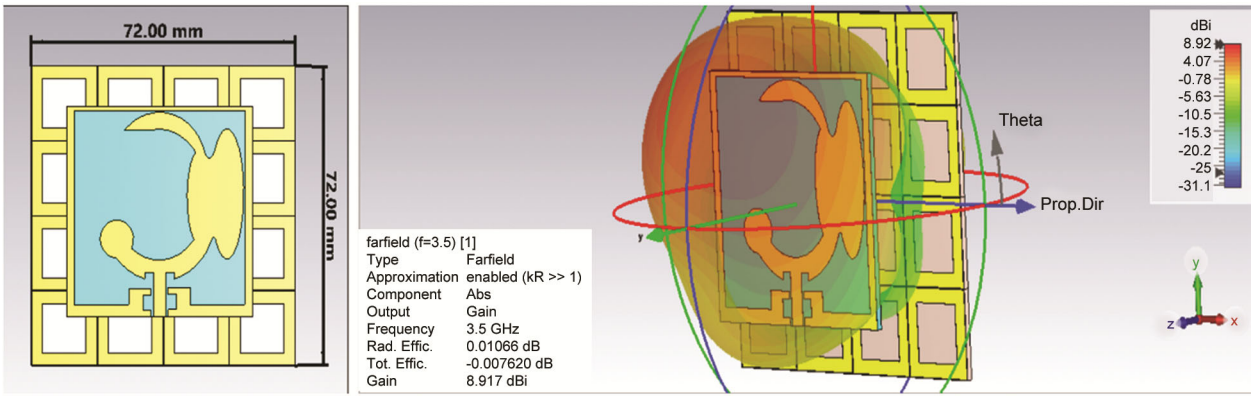

Fig. 4 — Proposed MP antenna inside CST simulation software: (a) MP antenna with FSS, (b) Gain with FSS

below the wideband (WB) monopole antenna with an air gap of 18 mm about $\frac{\lambda}{4}$.[22] When we embed the substrate of FSS at this optimised gap, the directivity of the antenna increases greatly. This enhancement is mainly explained by the beneficial reflection and surface current interaction between the monopole antenna and the conducting ground layer underneath. Therefore, antenna gain also rises significantly to 8.90 dB, which is reflected in Fig. 4(b).

Results and Discussion

This section of the paper presents and discusses the obtained results for the proposed antenna structure, including the antenna return loss (S_{11}), antenna gain, and radiation pattern.

Simulation Results

To assess the effect of the FSS on the performance of the antenna, a set of simulations was conducted and summarized in Fig. 5. The simulated S_{11} response between the antenna with no FSS (WO-FSS) layer and the antenna with FSS (W-FSS) are depicted in Fig. 5(a). The simulation results indicate that the addition of the FSS substrate results in improved impedance matching and enhanced reflection characteristics across the entire operating band. The simulated gain as presented in Fig. 5(b) shows that the antenna gain improves significantly with the introduction of the FSS. The improvement in gain associated with the introduction of the FSS is due to the FSS suppressing surface waves, which ultimately suppresses leakage radiation from the ground plane. This directs more energy to the intended radiation direction, thereby improving the overall gain. The effects of the FSS on radiation characteristics are presented in Fig. 5(c), which illustrates the radiation pattern at 3.5 GHz for both W-FSS and WO-FSS

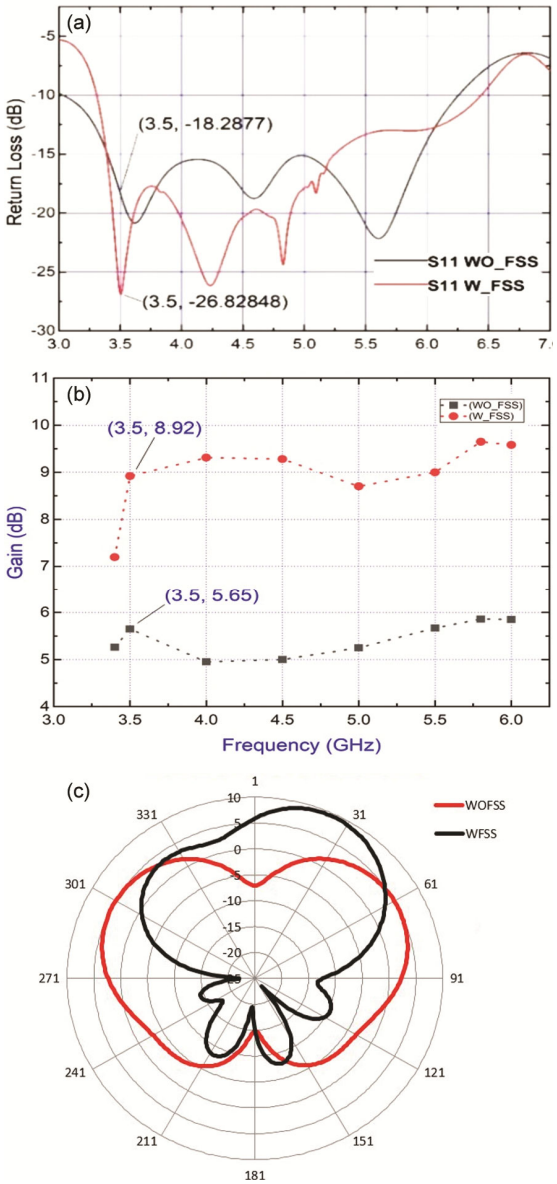

Fig. 5 — Simulated performance of the proposed antenna: (a) S_{11}, (b) Gain, (c) Radiation pattern –with and without FSS for 3.5 and 5.8 GHz respectively

cases. The MP antenna exhibits its normal quasi-omnidirectional characteristics without the FSS, featuring a wide main lobe and a moderate beamwidth, and is relatively isotropic in both the azimuth and elevation planes. When the FSS is introduced, the radiation pattern becomes more directional, with the power radiated in the main lobe increasing substantially. This improvement enhances gain while providing beamwidth control, offering flexibility to focus the antenna or radiate more broadly, depending on the applications, such as fixed wireless power transfer. Overall, the results substantively demonstrate that the FSS substrate has positively affected both impedance matching and radiation efficiency, validating the design of the proposed work.

Measurement Results

The designed microstrip patch antenna was evaluated within a controlled anechoic chamber, specifically designed to eliminate external electromagnetic interference and provide a highly stable measurement environment. This setup is crucial, considering the role of microstrip patch antennas in high-frequency applications where reliable radiation characteristics are paramount. For the assessment, the experimental arrangement included the fabricated antenna prototype, a calibrated Keysight PNA Network Analyzer (Model N5221B, covering 10 MHz to 13.5 GHz), a spectrum analyzer, as well as high-quality RF cables and connectors. The anechoic chamber itself played a key role in maintaining measurement integrity. Before testing, the chamber underwent thorough calibration to ensure minimal electromagnetic interference. Following this, the antenna was connected to the network analyzer using precisely matched RF cables, thereby supporting accurate and repeatable characterization of the antenna's performance.

Once the experimental setup was complete, we performed return-loss measurements for the antenna in two configurations: first case, WO-FSS layer and the second, W-FSS. The measured results closely tracked the simulations, which strongly supports the accuracy of both the design and the fabrication process. For additional validation, we assessed the antenna's gain at two independent research labs: the Antenna Laboratory for 5G Mobile Communication, Wireless Communication Centre Universiti Teknologi Malaysia (UTM), and the Antenna Research Centre Universiti Teknologi MARA (UiTM). By conducting measurements at both facilities, each employing its own automated systems, this is to ensure the consistency and reliability of the antenna's performance across different test environments.

The comparative results are summarised in Fig. 6, which presents the experimental results. The measured S_{11} response with and without the FSS reflector are shown in Fig. 6(a). In both simulations and prototype measurements, the impedance is perfectly matched.

Following that, Fig. 6(b) represents the gain behaviour of both of them, where the WO-FSS attained 5 dB at 3.5 GHz and with the addition of FSS, the gain attained 8.15 dB at 3.5 GHz, with a peak of

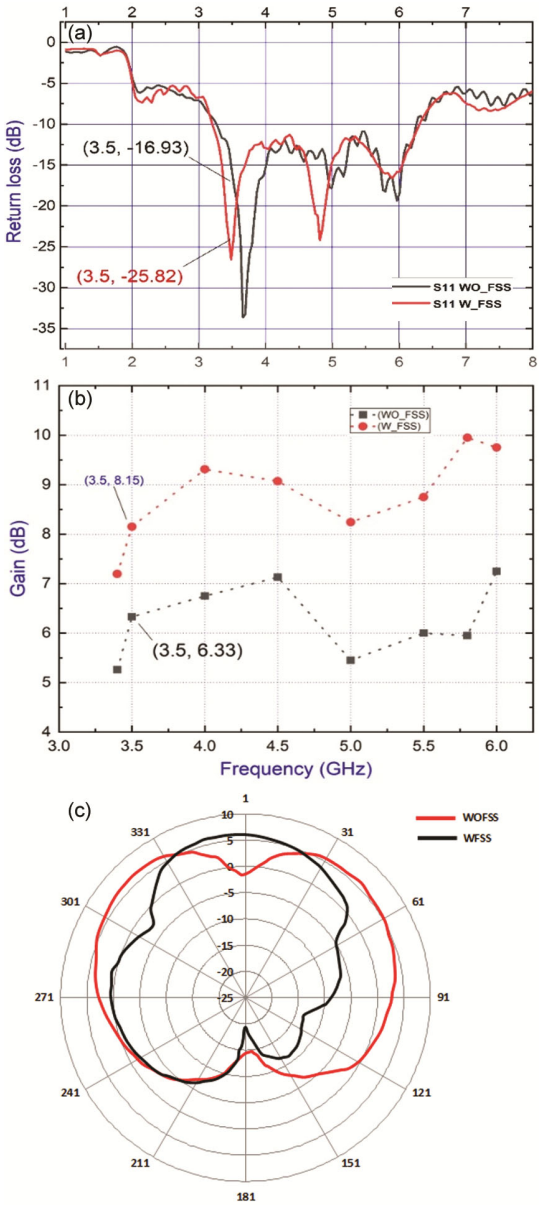

Fig. 6 — Experimental results of the proposed MP antenna: (a) S_{11}, (b) Gain, (c) Radiation pattern with and without FSS for 3.5 and 5.8 GHz respectivly

approximately 10 dB at 5.8 GHz. Lastly, Fig. 6(c) represents the radiation patterns at 3.5 and 5.8 GHz as measured respectively. The antenna readiation W-FSS case demonstrates enhanced directivity and beam shaping with higher asymmetry, whilst the WO-FSS case preserves a smoother and more symmetric omnidirectional profile (with a distinct main lobe and smaller side lobes). All these findings confirm that the FSS layer reinforces the performance of the antenna through advances in impedance matching, gain, and radiation directivity, hence validating the high correlation between the results of the simulation and the results of the measurements.

Results Comparison

A comparison of the proposed FSS-loaded UWB antenna with existing high-gain designs as given in Table 2, shows it to be more compact with a lower profile and volume. It also offers improved bandwidth and gain, making it well-suited for size-sensitive 5G and 6G applications. The single-layer FSS design simplifies manufacturing compared to bulkier, costlier multi-layer alternatives.

Rectifier Circuit Simulation and Fabrication Process

After completing the antenna simulation and fabrication, a rectifier circuit was designed and simulated using ADS software to convert the received RF signal into DC voltage for powering a load. If the signal voltage is low, amplification via a booster or buck converter can be employed.[35] The goal is to develop a rectifier for a wireless sensor with high power conversion efficiency, wide dynamic range, and strong sensitivity. Design considerations included application requirements, efficiency, frequency, output voltage/current, cost, and complexity. A voltage doubler was selected for its simplicity and effectiveness in converting AC to DC, functioning like a full-wave bridge to utilize both signal cycles.[36] Impedance matching between the 50 Ω antenna and rectifier is achieved using microstrip lines or stubs, which also filter out unwanted harmonics. Stub dimensions are optimized for minimal return loss at the resonant frequency. This approach is preferred over band-pass filters due to lower design complexity. The simulated rectifier and matching circuit in ADS are shown in Fig. 7. Schottky diodes are used in rectifier circuits due to their low threshold voltage and low junction capacitance, which enable efficient operation at low power and high frequencies. The HSMS-2850 model is selected for its fast switching and low forward voltage, making it ideal for energy harvesting applications. However, the diode's nonlinear characteristics can complicate impedance matching. A voltage doubler is chosen to balance efficiency and simplicity in the rectifier design.

Impedance matching between the 50 Ω antenna and rectifier is achieved using microstrip transmission lines, optimized via the Smith chart and LineCalc tools in ADS software. Matching accuracy is critical, as any mismatch can reduce conversion efficiency and

Table 2 — Results comparison of the proposed work with other studies

Year	Operational bandwidth (GHz)	Gain (dB)	Maximum gain (dB)	Number of FSS layers	Key Findings
2020	3.1 to 15	4.9	10.9	Single	High gain, no specific limitations mentioned[23]
2020	3 to 11.9	3.65	7.8	Single	Lossy FR4 limits efficiency at high frequencies; low gain (3–6 GHz)[24]
2013	3.6 to 3.9	4	6	Single	Narrow bandwidth, low gain (2–3.7 GHz)[25]
2019	2.9 to 9.3	3	8	Single	FSS improves gain but no bandwidth enhancement; reduced gain from E to T shape[26]
2021	3.6 to 6.1	3.8	7.87	Single	Large FSS layer; reduced efficiency above 5 GHz (4.9 GHz)[27]
2020	3 to 12	2.8	6.6	Single	Low directivity without FSS; mismatch causes performance issues[28]
2019	3.1 to 18.6	2.7	6.9	Single	Large FSS layer; discrepancies between simulated and theoretical frequencies[29]
2022	2.5 to 11	2–5	8.6	Single	High FR-4 dielectric loss; low gain at sub-5 GHz.[30]
2020	3.16 to 15	4	8.9	Single	High dielectric loss limits performance at higher frequencies.[31]
2016	3 to 14.6	4.5	8.7	Double	Dual-layer FSS increases complexity; moderate gain (8.5 dB) in GPR applications.[32]
2018	3.05 to 13.4	4.2	8.5	Double	Dual-layer FSS increases complexity and cost; achievable 8.5 dB gain with single layer.[33]
2021	3 to 21	4.8	7.2	Multi-Layer	FR-4 loss affects performance; multi-layer FSS increases complexity and cost.[34]
This Work	3 to 6.5	5 @ 3.5 GHz	8.15 @ 3.5 GHz & 10 @ 5.8 GHz	Single	High gain with single-layer FSS; easy fabrication, low complexity, broad bandwidth.

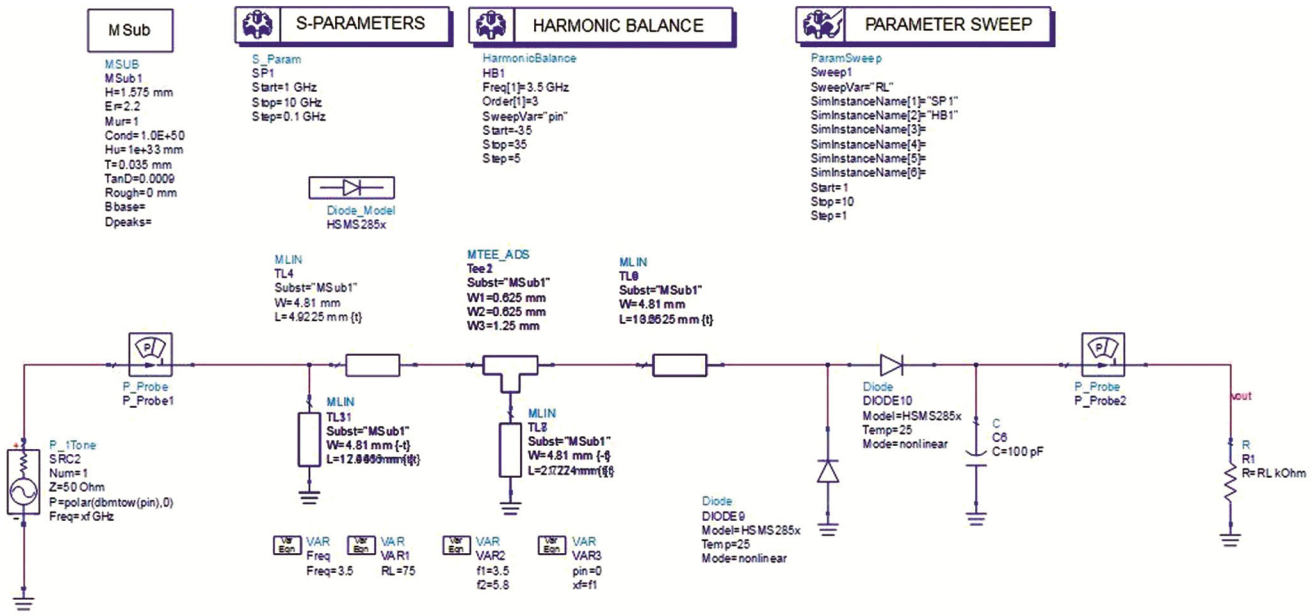

Fig. 7 — Schematic diagram of the proposed rectifier with impedance matching network

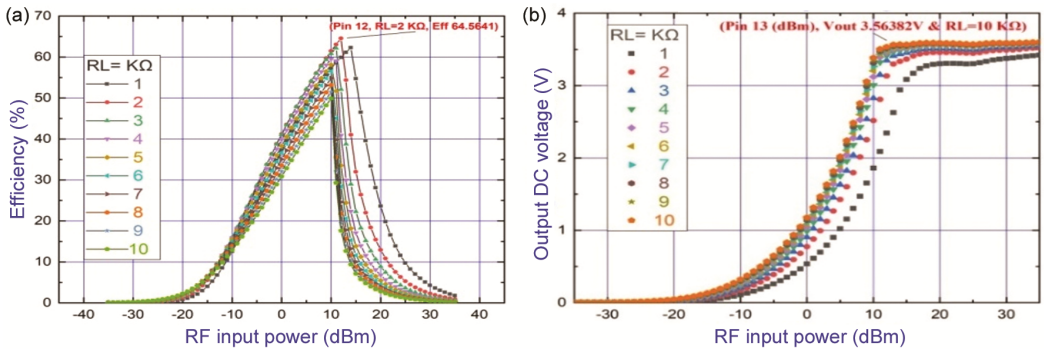

Fig. 8 — Simulated rectifier PCE and output voltage: (a) PCE Vs RF input power, (b) output D.C voltage Vs resistive load

output voltage.[37] To improve power transfer and minimize circuit size, a Pi-section matching network connects the RF source to the rectifier.[38] The transmission line dimensions are calculated to match the rectifier at 3.5 GHz. The design is optimized using optimize tool inside ADS software for both 3.5 and 5.8 GHz using microstrip lines and capacitors (10–100 pF), achieving high power conversion efficiency with a 2 kΩ load and 100 pF parallel capacitor. The rectifier's performance, including power conversion efficiency and DC output voltage, is simulated in ADS by varying input RF power from –35 dBm to 35 dBm. It is demonstrated in Fig. 8 that rectifier efficiency and output voltage are dependent on the resistive load and input power. Peak efficiency of 64% occurs at 12 dBm input power with a 2 kΩ load, while the highest DC output of 3.5 V is reached at 13 dBm with a 10 kΩ load.

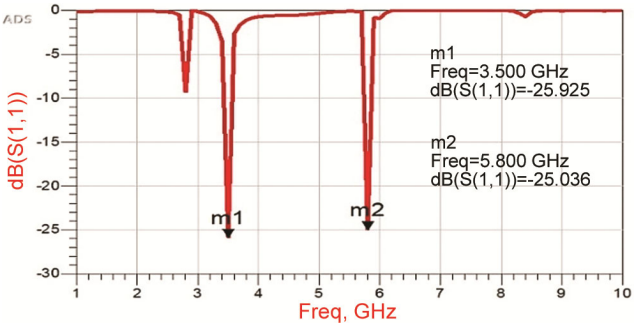

Fig. 9 — Simulated return loss rectifier circuit results

There is a trade-off: higher loads increase voltage but reduce efficiency, requiring careful load selection based on application needs. The rectifier is well-suited for low-power wireless sensor and IoT applications, which typically require 1–3 V. With over 3 V output and high sensitivity enabled by a high-gain FSS antenna, it supports battery-free operation in remote areas. Dual-band S_{11} response at 3.5 and 5.8 GHz as shown in Fig. 9

Table 3 — Proposed rectifier circuit comparison with other studies in terms of frequency, efficiency, and output voltage

Year	Frequency (GHz)	Substrate	Antenna Type	Total Dimensions (mm × mm)	PCE	Output DC Voltage	Key Findings
2019	28-38	Rogers 5880	Copper	NA	42-46%	N/A	Low efficiency, output voltage not mentioned, mismatch between simulation and measurement results. [39]
2015	2.45	FR4	NA	NA	6.3%	2500 mV	Conversion efficiency of 6.3% at 0 dBm input, PCE not included. [40]
2020	0.9, 1.8, 2.45	FR4	NA	NA	46%	N/A	Complex design, low PCE, output voltage not included. [41]
2021	2.45	FR4	NA	NA	73.13%	6.651 V	Theory-based only, high input power; erroneous equation for calculating rectifier efficiency, mismatch in S_{11}. [42]
2022	3.5	RT/Duroid 5880	NA	NA	42.5%	N/A	Low efficiency, output voltage not included, based on another published paper (ambiguous).[43]
2019	2.4 and 3.5	FR4	NA	NA	39.6%	N/A	High input power, low efficiency. [44]
2020	3.5 and 5.8	RT/Duroid 5880	Patch	NA	44%	656.88 mV	Low efficiency and output voltage. [45]
2019	3.5	Rogers RT6002	Patch	47 × 46.75 × 0.76 mm³	29.72%	1.5 V	Low efficiency, issues with power scaling. [46]
This Work	3.5	Rogers 5880	Patch	50 × 50	64.5%	3.5 V @ 13 dBm	Wide power dynamic range, acceptable output voltage, and efficiency.

is allowing efficient RF energy harvesting even when 5G signals are unavailable.

The proposed rectifier is simulated inside ADS software and fabricated using Rogers substrate with 1.575 mm of thickness to evaluate its effectiveness. Finally, the proposed rectifier circuit is compared with several related studies in Table 3 below. It draws attention to important factors like frequency range, substrate type, antenna type, Power Conversion Efficiency (PCE), output DC voltage, and the noteworthy results of each investigation. This comparison, which focuses on efficiency, output voltage, and general design considerations, attempts to shed light on the performance characteristics of the suggested design concerning current rectifier circuits. This highlights the enhancements made in the current work, especially regarding efficiency and power dynamic range.

Conclusions

This paper introduces the design, simulation, optimization, and fabrication of a modified MP antenna and an integrated rectifier circuit aimed at energy harvesting for low-band 5G communications. The single FSS reflector was added underneath the antenna to improve performance. This resulted in a notable gain increase of 3.5 dB at 3.5 GHz, for a total gain of 10 dB at a resonant frequency of 5.8 GHz. The effectiveness of the suggested design was demonstrated by the good match between the simulation results and the manufactured prototype. The rectifier circuit was designed to operate efficiently over a broad power dynamic range of −35 to 35 dB, with a 3.5 V output at 13 dBm of transmitted power. This makes it appropriate for low-power applications like wireless sensors and Internet of Things devices. Due to its enhanced efficiency and performance, this integrated system may find use in impulse radar systems, microwave imaging, and short-range wireless communication networks. Future research will concentrate on measuring the prototype and integrating it with the antenna in order to assess the rectenna system's overall effectiveness and performance.

Acknowledgements

The authors are very thankful to the University Tenaga National (Uniten) for this work funded under grant UNITEN NEC Grant (J510051171).

References

1 Goyal J, Singla K, Akashdeep & Singh S, A survey of wireless communication technologies from 1G to 5G, *Lect Notes Data Eng Commun Technol*, **44** (2020) 885–894, doi: 10.1007/978-3-030-37051-0_69.

2 Muppavaram K, Govathoti S, Kamidi D & Bhaskar T, Exploring the generations: A comparative study of mobile technology from 1G to 5G, *Int J Electron Commun Eng*, **10(7)** (2023) 54–62, doi: 10.14445/23488549/IJECE-V10I7P106.

3 Sufyan A, Khan K B, Khashan O A, Mir T & Mir U, From 5G to beyond 5G: A comprehensive survey of wireless

network evolution, challenges, and promising technologies, *Electronics*, **12(10)** (2023) 2200, doi: 10.3390/electronics12102200.
4 Taha B S, Design of quad band microstrip patch antenna for electromagnetic energy harvesting applications, *J Southwest Jiaotong Univ*, **54(5)** (2019),
5 Mahmood A A, Kadhim A A & Al-raweshidy H S, Transmission of physical layer network coding based on massive MIMO over millimeter wave channel, *Iraqi J Inf Commun Technol*, **6(2)** (2024) 31–41, doi: 10.31987/ijict.6.2.220.
6 Abdalrazak M Q, Majeed A H & Abd-Alhameed R A, An analytical investigation on the performance of 1D and 2D antenna arrays for MM-wave modern communication systems, *Iraqi J Inf Commun Technol*, **6(2)** (2024) 78–88, doi: 10.31987/ijict.6.2.254.
7 Nwalike E D, Ibrahim K A, Crawley F, Qin Q, Luk P & Luo Z, Harnessing energy for wearables: A review of radio frequency energy harvesting technologies, *Energies*, **16(15)** (2023) 5711, doi: 10.3390/en16155711.
8 Rana M S, Mistry P, Rahaman M J, Shipon S I, Ovi S Z H, Rana M M & Fahim T A, At 28 GHz microstrip patch antenna for wireless applications: A review, *TELKOMNIKA*, **22(2)** (2024) 251–262.
9 Kumar A & Chadhar R M, A review paper of microstrip patch antenna design and its application, *Int J Recent Dev Eng Technol*, **13(4)** (2024), ISSN: 2347–6435.
10 Sharma P & Singh A K, A survey on RF energy harvesting techniques for lifetime enhancement of wireless sensor networks, *Sustain Comput Inform Syst*, **37** (2023) 100836.
11 Anwar R S, Mao L & Ning H, Frequency selective surfaces: A review, *Appl Sci*, **8(9)** (2018) 1689, doi: 10.3390/app8091689.
12 Shi C, Zou J, Gao J & Liu C, Gain enhancement of a dual-band antenna with the FSS, *Electronics*, **11(18)** (2022) 2882, doi: 10.3390/electronics11182882.
13 Albaihani Y, Akram R, Almohaimeed Z, Almohaimeed A & Hajlaoui E A, Optimal antenna design for wireless energy harvesting system in ISM band, *Results Phys*, (2025) 108255, doi: 10.1016/j.rinp.2025.108255.
14 Fatima F, Akhtar M J & Ramahi O M, Frequency selective surface structures-based RF energy harvesting systems and applications: FSS-based RF energy harvesting systems, *IEEE Microw Mag*, **25(3)** (2024) 47–69, doi: 10.1109/MMM.2023.3340988.
15 Alsudani A & Marhoon H M, Design and enhancement of microstrip patch antenna utilizing mushroom like-EBG for 5G communications, *J Commun*, **18(3)** (2023) 156–163, doi: 10.12720/jcm.18.3.156-163.
16 Taha B S & Marhoon H M, Simulation and manufacturing of modified circular monopole microstrip antenna for UWB applications, *Int J Adv Appl Sci*, **2252** (2021) 8814.
17 Thakur E, Kumar D, Jaglan N, Gupta S D & Srivastava S, Mathematical analysis of commonly used feeding techniques in rectangular microstrip patch antenna, in *Advances in Signal Processing and Communication*, edited by B Rawat, A Trivedi, S Manhas & V Karwal (Springer) 2019, 27–35.
18 Alsudani A & Marhoon H M, Performance enhancement of microstrip patch antenna based on frequency surface substrate for 5G communication applications, *J Commun*, **17(10)** (2022) 851–856, doi: 10.12720/jcm.17.10.851-856.
19 Kumar A, De A & Jain R K, Gain enhancement using modified circular loop FSS loaded with slot antenna for Sub-6GHz 5G application, *Prog Electromag Res Lett*, **98** (2021) 41–49.
20 Kamel A S & Jalal A S, Reconfigurable monopole antenna design based on fractal structure for 5G applications, *Iraqi J Inf Commun Technol*, **1(1)** (2021) 177–186, doi: 10.31987/ijict.1.1.159.
21 Awan W, Choi D M, Hussain N, Elfergani I, Park S G & Kim N, A frequency selective surface loaded UWB antenna for high gain applications, *Comput Mater Contin*, **73** (2022) 6169–6180.
22 Muppavaram K, Govathoti S, Kamidi D & Bhaskar T, Exploring the generations: A comparative study of mobile technology from 1G to 5G, *Int J Electron Commun Eng*, **10(7)** (2023) 54–62, DOI: 10.14445/23488549/IJECE-V10I7P106
23 Varshney A & Gençoglan D N, High-gain multi-band Koch fractal FSS antenna for Sub-6 GHz applications, *Appl Sci*, **14(19)** (2024) 9022, doi: 10.3390/app14199022.
24 Marhoon H M & Qasem N, Simulation and optimization of tuneable microstrip patch antenna for fifth-generation applications based on graphene, *Int J Electr Comput Eng*, **10(5)** (2020) 5546–5558.
25 MohdYunus N H, Sampe J, Yunas J, Pawi A & Rhazali Z A, MEMS based antenna of energy harvester for wireless sensor node, *Microsyst Technol*, **26** (2020) 2785–2792.
26 Taha B S, Marhoon H M & Naser A, Simulating of RF energy harvesting micro-strip patch antenna over 2.45 GHz, *Int J Eng Technol*, **7(4)** (2018) 5484–5488, doi: 10.14419/ijet.v7i4.27031.
27 MohdYunus N H, Yunas J, Pawi A, Rhazali Z A & Sampe J, Investigation of micromachined antenna substrates operating at 5 GHz for RF energy harvesting applications, *Micromachines*, **10(2)** (2019), doi: 10.3390/mi10020146.
28 Taha B & AlSharabati T, Performance comparison between the FR4 substrate and the Rogers Kappa-438 substrate for microstrip patch antennas, *Int J Comput Sci Mob Comput*, **9(2)** (2020) 1–12.
29 Marhoon H M, Design and optimisation of microstrip bowtie antenna based on graphene material for terahertz applications, *Politeknik Dergisi*, **27(1)** (2022) 221–226, doi: 10.2339/politeknik.1056109.
30 Kushwaha N & Kumar R, Design of slotted ground hexagonal microstrip patch antenna and gain improvement with FSS screen, *Prog Electromag Res B*, **51** (2013) 177–199.
31 Mondal K, Bandwidth and gain enhancement of microstrip antenna by frequency selective surface for WLAN, WiMAX applications, *Sādhanā*, **44** (2019) 1–10.
32 Marhoon H M, Qasem N, Basil N & Ibrahim A R, Design and simulation of a compact metal-graphene frequency reconfigurable microstrip patch antenna with FSS superstrate for 5G applications, *Int J Eng Appl (IREA)*, **10(3)** (2022) 193–201.
33 Al-Gburi A J A, Ibrahim I M, Zakaria Z, Abdulhameed M K & Saeidi T (2021), Enhancing gain for UWB antennas using FSS: A systematic review, *Mathematics*, **9(24)** 3301, doi: 10.3390/math9243301

34 Yuan Y, Xi X & Zhao Y, Compact UWB FSS reflector for antenna gain enhancement, *IET Microw Antennas Propag*, **13** (2019) 1749–1755.

35 Byun S J, Jang B G, Jo J W, Choi D Y, Pu Y G, Yoo S S, Kim S K, Jung Y J & Lee K Y, Design of a high efficiency bi-directional four-switch buck-boost converter with HV gate driver for multi-cell battery power bank applications, *IEEE Open J Circuits Syst*, **6** (2025) 110–119, doi: 10.1109/OJCAS.2025.3557835.

36 Choong F C M & May Y Y, An improved DC-DC boost converter for energy harvesting, *J Eng Technol Appl Phys*, **5(2)** (2023) 69–78, doi: 10.33093/jetap.2023.5.2.

37 Lee Y C, Ramiah H, Choo A, Churchill K K P, Lai N S, Lim C C, Chen Y, Mak P I & Martins R P, High-performance multiband ambient RF energy harvesting front-end system for sustainable IoT applications: A review, *IEEE Access*, **11** (2023) 11143–11164, doi: 10.1109/ACCESS.2023.3241458.

38 Reddafa A & Boudjerda M, Modeling of Schottky diode and optimal matching circuit design for low power RF energy harvesting, *Heliyon*, **10(6)** (2024) e27792, doi: 10.1016/j.heliyon.2024.e27792.

39 Kundu S, High gain compact ultra-wideband antenna-frequency selective surface and its performance evaluation in proximity of soil surface, *Microw Opt Technol Lett*, **63** (2021) 869–875.

40 Alamayreh A, Qasem N & Rahhal J S, General configuration MIMO system with arbitrary OAM, *Electromagnetics*, **40(5)** (2020) 343–353, doi: 10.1080/02726343.2020.1780378.

41 Fırat E, Oral A & Erbaş C D, Design of a rectangular slotted microstrip patch antenna for C band radar applications, *Proc 7th Glob Power Energy Commun Conf (GPECOM)* (Bochum, Germany) 2025 974–978, doi: 10.1109/GPECOM65896.2025.11061830.

42 Kumar T & Kumar V, Bandwidth and gain enhancement of a rectangular metasurface microstrip patch antenna, *Proc 1st Int Conf Electron Commun Signal Process (ICECSP)* (New Delhi, India) 2024, 1–4, doi: 10.1109/ICECSP61809.2024.10698191.

43 Elias B B Q, Ismail M M, Alanssari A I, Rhazali Z A, Soh P J, Misran H, Bashar B S, A metasurface-based high-gain patch antenna for future multiband wireless communication, *Iraqi J Inf Commun Technol*, **7** (2024) 47–60, doi:10.31987/ijict.7.1.268.

44 Mondal R, Reddy P S, Sarkar D C & Sarkar P P, Compact ultra-wideband antenna: Improvement of gain and FBR across the entire bandwidth using FSS, *IET Microw Antennas Propag*, **14** (2020) 66–74.

45 Yuan Y, Xi X & Zhao Y, Compact UWB FSS reflector for antenna gain enhancement, *IET Microw Antennas Propag*, **13** (2019) 1749–1755.

46 Ray S, Haldar S, Sanyal R, Routh K, Kundu R & Chatterjee N, Design and analysis of an ultra-wideband frequency selective surface for 5G communication systems and spatial filtering applications, *Proc 8th Int Conf Electron Mater Eng Nano Technol (IEMENTech)* (Kolkata, India) 2025, 1–5, doi: 10.1109/IEMENTech65115.2025.10959684.